eor.istanbul.edu.tr

Official Publication of Istanbul University Faculty of Dentistry

Eur Oral Res 2023; 57(3): 128-132

Original research

Evaluation of submandibular gland and submandibular fossa: A combined cone beam computed tomography and ultrasound study

Esin Akol Görgün[1], **Fatma Çağlayan**[1]

Purpose
The purpose of this study was to use Cone Beam Computed Tomography (CBCT) to evaluate the submandibular fossa (SF) morphometrically and ultrasonography (USG) to evaluate the submandibular gland (SG).

Materials and Methods
Radiological evaluation was performed on 40 SFs and SGs from 20 patients. The depth and width of the SF were measured on axial CBCT sections, while the antero-posterior, medio-lateral, and supero-inferior lengths and volumes of the SGs were measured by USG. Statistical analysis was performed to evaluate CBCT and USG measurements.

Results
The study found a statistically significant positive correlation between SF depth and SG medio-lateral dimension ($p = 0.023$), SF width and SG antero-posterior dimension ($p = 0.021$), and SF width and SG volume ($p = 0.000$). However, there was no significant correlation between SF depth and SG volume ($p=0.146$).

Conclusion
The SF is an important area in surgical procedures planned in the mandibular posterior region, especially in implant applications. The dimensions of the SF are closely related to the dimensions of the SG. USG can be used to examine the SG without the risk of ionizing radiation.

Keywords: *Submandibular gland, submandibular fossa, ultrasonography, cone beam computed tomography, implant surgery*

Introduction

Submandibular fossa (SF) is a common anatomical variation that occurs because of the pressure of the submandibular salivary gland on the lingual cortex of the mandible body. It starts from the distal of the mental foramen inferior to the mylohyoid line and extends to the mandibular third molars. The submandibular gland is located in this region. Various imaging methods such as panoramic radiography, Cone Beam Computed Tomography (CBCT), and Computed Tomography (CT) have been used to evaluate this region (1-4).

Ultrasonography (USG) is a noninvasive and easy-to-apply imaging method that does not involve the risk of ionizing radiation. It is used to examine muscles, tendons, joints, vessels, and internal organs that are not behind the bone. Due to the superficial location and appropriate homogeneous soft tissue densities of the salivary glands, USG is the preferred imaging technique for their evaluation (5).

CBCT is a convenient imaging method for the three-dimensional evaluation of the bony structures of the maxillofacial region. It provides

ORCID IDs of the authors: E.A.G. 0000-0002-6711-7188; F.Ç. 0000-0002-0666-8824

[1]*Department of Oral Dental and Maxillofacial Radiology, Faculty of Dentistry, Ataturk University, Erzurum, Turkiye*

Corresponding Author: Fatma Çağlayan

E-mail: facagla@gmail.com

Received: 26 April 2022
Revised: 28 November 2022
Accepted: 11 December 2022

DOI: 10.26650/eor.20231109135

How to cite: *Akol Gorgun E, Caglayan F. Evaluation of submandibular gland and submandibular fossa: A combined tomography and ultrasound study. Eur Oral Res 2023. Eur Oral Res 2023; 57(3): 128-132.* DOI: 10.26650/eor.20231109135

high-quality images with low millimeter resolution and low radiation dose (6-13). Different methods have been used to measure SF depth in CBCT in various studies in the literature (1, 3, 14). For instance, Parnia *et al.* (14) determined the most prominent upper and lower points of the lingual concavity corresponding to the submandibular fossa in paraxial sections and drew a starting line connecting them. They then measured the SF depth by drawing a second line perpendicular to the first line from the deepest point of the fossa. In some studies, SF depth was measured on cross-section CBCT images by drawing a line to the most prominent upper and lower points of the lingual concavity and a second line from the deepest point of the concavity to the first line (1, 3).

Implant treatment has become very popular in the rehabilitation of missing teeth. One of the most important structures to be examined before placing an implant in the mandible is the depth of the SF. Damage to the SF due to lingual plate perforation during surgery can result in severe bleeding and subsequent hematoma with life-threatening consequences due to upper airway obstruction.

Since the SG is located in the SF, the depth of the SF should be related to the dimensions of the submandibular gland. However, there are no studies on this subject in the literature. The aim of this study was to evaluate the SF by CBCT and the SG by USG and to investigate whether there was a relationship between the SG size and SF dimensions measured by USG and CBCT, respectively. The null hypothesis tested in this study is that no correlation could be established among measurements made with either device.

Materials and Methods

Ethical approval

This study was conducted at the Department of Oral and Maxillofacial Radiology, and its compliance with scientific ethical standards was approved by the faculty ethics committee's decision numbered 2021/58. Informed consent forms were obtained from the patients.

Sample size estimation

The sample size for the Pearson correlation test, which was used to test the primary hypothesis of the study, was calculated. As a result of the sample size analysis performed using Cohen's effect size value of 0.50, it was determined that a minimum of 29 individuals should be included in the study ($1 - \beta = 0.80$) to reveal significant differences between the groups with 80% power and $\alpha = 0.05$ error (95% confidence interval). CBCT and USG were used to evaluate 40 SFs and SGs of these patients, respectively.

Study design

The patients were randomly selected among those who applied to the Department of Oral and Maxillofacial Radiology for CBCT scans for various reasons in 2021, and the study took one year to complete. When selecting the patients, the absence of mandibular bone destruction caused by pathology, complete visualization of the mandible, and the patients' voluntary participation were taken into consideration.

CBCT procedures and measurements

In the study, 40 SFs of 20 patients were included, who were examined with a flat panel NewTom 3G Dental Volumetric Tomography device (NewTom FP, Quantitative Radiology, Verona, Italy). The device had a voxel size of 0.16 mm and a typical exposure time of 5.4 seconds, and it operated with the conical beam technique at 110 kVp as standard and a maximum of 15 mA. The device had an automatic exposure control system (AEC), which adjusted the dose and exposure time according to the density of the patient's skull in the guide image obtained at the beginning of the shooting. The study reconstruction was obtained with axial sections at 0.5 mm intervals of the patients whose raw data were obtained, and it was set parallel to the lower border of the mandible.

The depth of the submandibular fossa was measured on the axial section where the fossa was seen the deepest. A line was drawn on the lingual surface of the mandible on the axial section where the fossa was the deepest, connecting the anterior and posterior borders of the fossa. The length of this line was measured and recorded as the SF width. Then, a perpendicular line was drawn from the first line to the deepest point of the fossa to measure and record the SF depth (Figure 1)

USG procedures and measurements

The submandibular salivary glands of individuals who had undergone CBCT imaging for various reasons were examined using USG with their informed consent. The USG evaluation was performed using a Toshiba Aplio 300 ultrasonography device (Toshiba Corporation, Tokyo, Japan) and a 12-MHz linear array transducer probe. During the USG examination, the patient's head was fixed in extension, and the SG was first examined transversely and then the probe was

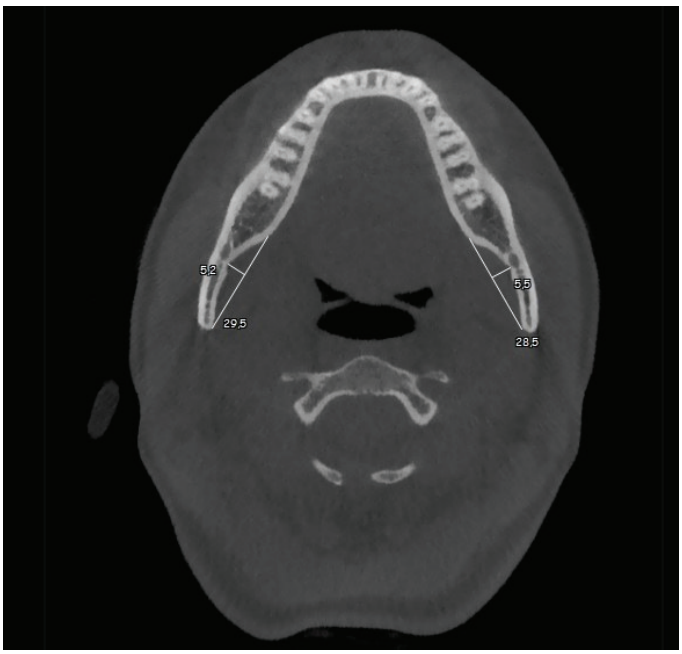

Figure 1. *Measurement of submandibular fossa width and depth on the axial CBCT section. The width of the SF was measured by connecting the anterior and posterior borders of the fossa. The depth of the SF was measured with a perpendicular line to the deepest point of the fossa from the first line.*

rotated longitudinally to calculate the volume of the submandibular salivary gland (Figure 2).

To begin the USG examination, the probe was positioned parallel to the lower edge of the mandible after locating the submandibular salivary gland. The homogeneous echogenic structure of the SG parenchyma could be easily distinguished from the surrounding soft tissues using USG. To make dimensional measurements, the CALIPER option was selected on the USG device. The image was frozen when the SG was displayed in full on the USG screen. Distance 1, which represented the antero-posterior length of the SG, was measured and recorded (Figure 3). Similarly, the supero-inferior measurement was made on the same image and recorded as distance 2 (Figure 4). The probe was then turned perpendicular to the body of the mandible to measure the medio-lateral length of the submandibular gland, which was recorded as distance 3. Finally, the VOLUME icon was clicked on the touch screen of the device to calculate the volume of the SG automatically (Figure 4).

Statistical analysis

The statistical analysis was performed using the IBM SPSS Statistics 20 package program (Armonk, NY: IBM Corp., USA). Descriptive statistics were utilized to determine the distribution of the data, and the conformity of all values to the normal distribution was assessed. Pearson correlation coefficient was employed to evaluate the relationship between SF depth and medio-lateral length of SG, SF width and superior-inferior length of SG, and SF width and volume of SG. However, it was discovered that the antero-posterior length of SG did not exhibit normal distribution ($p<0.05$), and therefore, Spearman correlation coefficient was utilized to evaluate the relationship between SF width and antero-posterior length of SG. A significance level of $p<0.05$ was used for statistical significance. All measurements were conducted by the same observer with a minimum of 3 years of maxillofacial USG experience, and the reliability of the measurements was assessed using the intra-observer correlation test.

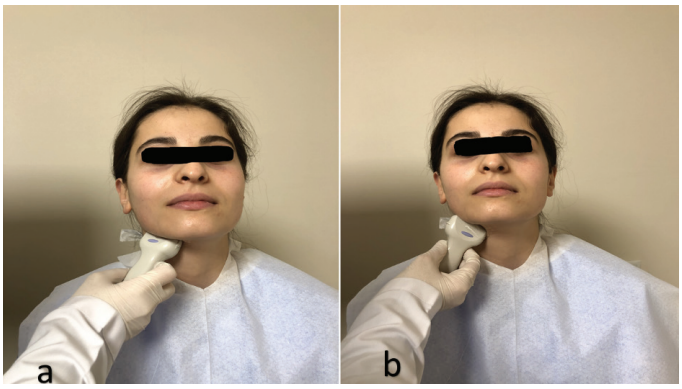

Figure 2. *Examination of submandibular gland by USG. a: Transversal direction, b: Longitidunal direction.*

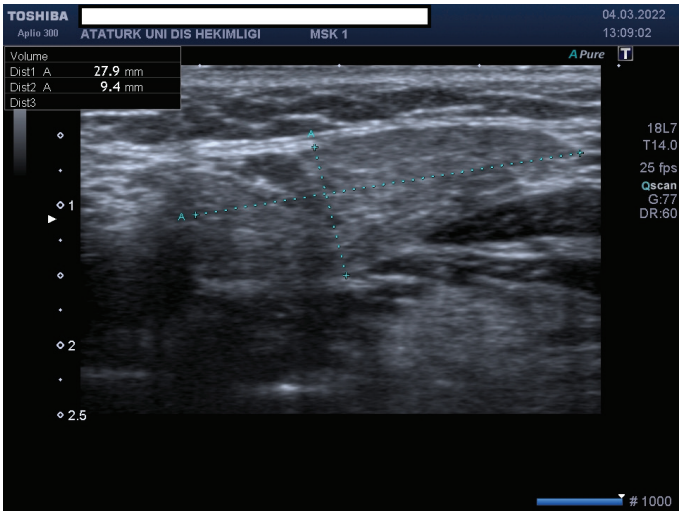

Figure 3. *The anteroposterior length of the submandibular gland was measured and recorded as distance 1. Supero-inferior measurement was also made on the same image and it was recorded as distance 2.*

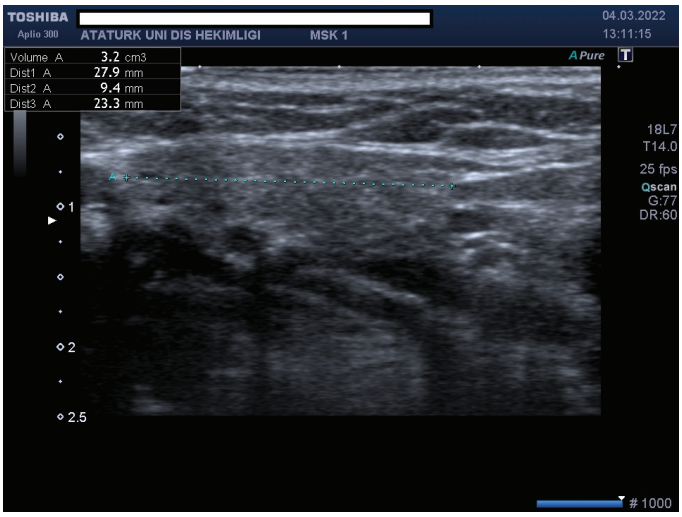

Figure 4. *To measure the third dimension, the probe was turned perpendicular to the body of the mandible and the medio-lateral length of the submandibular gland was measured and recorded as distance 3. After the dimension measurements in these three planes are done, the volume was calculated automatically.*

Results

The study included a total of 20 patients (6 men and 14 women) and examined 40 SF and SG. The participants had a mean age of 34.65±15.16. Cronbach's alpha values of 0.941 and 0.997 were obtained for the CBCT and USG measurements, respectively, which were used to assess intra-observer agreement (95% Confidence Interval). Table 1 presents the descriptive analysis of antero-posterior, supero-inferior,

Table 1. *The descriptive analyses of antero-posterior, supero-inferior, medio-lateral lengths, and volume of SG, SF depth and SF width.*

	n	Mean± SD
Antero-posterior length of SG	40	28.272±3.040 mm
Supero-inferior length of SG	40	11.175±2.138 mm
Medio-lateral length of SG	40	26.402±4.059 mm
Volume of SG	40	4.245±0.713 cm^3
SF depth	40	4.467±0.801mm
SF width	40	30.355±4.618 mm

SG: Submandibular Gland, SF: Submandibular Fossa, SD: standard deviation

Table 2. *Correlation coefficients and significance levels between SF depth and SG medio-lateral size, SF width and SG supero-inferior size, SF width and SG volume, and SF width and antero-posterior length of SG.*

	r[a]	p
SF depth and medio-lateral length of SG	0.358	0.023*
SF width and superior-inferior length of SG	0.365	0.021*
SF width and volume of SG	0.678	0.000**
	rho[b]	**p**
SF width and antero-posterior length of SG	0.414	0.008**

*SG: submandibular gland, SF: submandibular fossa, [a] Pearson correlation coefficient, [b] Spearman correlation coefficient, *p <0.05, **p <0.01).*

medio-lateral lengths, and volumes of the submandibular glands, SF depth, and SF width.

Table 2 shows that there is a positive correlation between the SF depth measured on CBCT and the medio-lateral length of SG measured by USG (p=0.023, r= 0.358), indicating that as the medio-lateral length of the SG increases, the depth of the SF increases. Similarly, a positive correlation was found between the SF width measured on CBCT and the antero-posterior and superior-inferior lengths measured by USG (p=0.021, r=0.365), indicating that as the antero-posterior and supero-inferior lengths of the submandibular gland increase, the SF width increases (p=0.008, rho= 0.414). Moreover, a positive correlation was found between SF width measured on CBCT and submandibular gland volume measured by USG (p=0.000, r=0.678), indicating that as the submandibular gland volume increases, the SF width increases. However, there was no significant relationship between SF depth and volume of SG.

Discussion

The submandibular gland is located in the posterior part of the submandibular triangle, and its size is approximately 30x35x15 mm. The borders of the submandibular triangle are formed by the anterior and posterior belly of the digastric muscle and the body of the mandible (15).

Many studies in the literature have measured SF depth using CBCT sections. Stratemann *et al.* (16) found less than 1% relative error between their CBCT measurements and physical measurements on the skull. Other studies have also emphasized CBCT as the gold standard (17, 18). While cross-sectional images have been used in many studies to measure SF depth on CBCT (1-3), Quirynen *et al.* (13) classified bone morphologies into three types and found that it may be inaccurate to work on cross-section images in individuals with type II and III bone morphologies. Therefore, our measurements were made on axial sections.

In edentulous patients, SF depth measured from cross-sectional sections may not reflect accurate facts, as the top of the fossa may be adjacent to the bone surface. Parnia *et al.* (14) excluded some cases from their retrospective study on CT images of 100 patients due to this issue. In our study, we also excluded edentulous patients. Additionally, no other study in the literature has measured the antero-posterior width of SF.

Gandage *et al.* (19) investigated the sensitivity and specificity of USG in evaluating the salivary glands and found high sensitivity (93.33%) and high specificity (98.07%). In our study, we used USG to measure the size and volume of the submandibular gland in three dimensions. We found statistically significant positive correlations between the medio-lateral length of the submandibular gland and the SF depth measured on the axial images, and between the antero-posterior and supero-inferior lengths of the submandibular gland and the SF width measured on the axial images. These results were expected based on anatomical considerations.

SF depth and width are important structures to consider in surgical procedures of the posterior mandible, particularly in planning implant treatments. Damage to the SF due to lingual plate perforation during surgery can result in severe bleeding followed by life-threatening hematoma due to upper airway obstruction (20, 21). Therefore, USG can be considered as an alternative to CBCT in cases where rapid assessment of SF depth is required, as it is practical, non-invasive, inexpensive, and radiation-free. Furthermore, USG can evaluate any focus of infection and regional lymph nodes in the region (22).

Dental implants have become increasingly popular in the rehabilitation of edentulism. However, incorrect planning before surgery can cause serious damage to anatomical structures and lead to life-threatening injuries. Mandibular lingual concavities are depressions formed on the bone by the submandibular and sublingual salivary glands (23). Imaging of the SG helps prevent cortical lingual plate perforation, allows preservation of vascular structures, and nerves (24). Although CBCT is undisputedly superior to USG in the morphological and morphometric evaluation of bone including SF before implant, it is expensive, takes time, and contains ionizing radiation. Therefore, USG can be considered as an alternative imaging method in the rapid evaluation of SF depth in patients with implant planned.

The most important limitation of the present study is the sample size. In the future, the sample size should be expanded by increasing the number of patients. However, no other study in the literature has investigated SF and SG in combination with USG and CBCT. As this is the first study in the literature to use CBCT and USG in combination, it may pave the way for more comprehensive studies in the future.

Conclusion

This study found a positive correlation between the size and volume of the submandibular gland measured by USG and the SF depth and width measured by CBCT. In cases where SF depth and width need to be examined, such as in implant treatment, it may be recommended to use USG in addition to CBCT imaging.

Türkçe Özet: *Submandibuler bez ve submandibular fossanın değerlendirilmesi: Kombine konik ışınlı bilgisayarlı tomografi ve ultrason çalışması. Amaç: Bu çalışmanın amacı Konik Işınlı Bilgisayarlı Tomografi (KIBT) ile SF'yi morfometrik olarak ve Ultrasonografi (USG) ile SB'yi değerlendirmektir. Gereç ve Yöntem: Çalışma kapsamında 40 SF ve 20 hastanın SB'leri radyolojik olarak değerlendirildi. İskeletsel olarak, SF'nin derinliği ve genişliği aksiyal KIBT kesitlerinde ölçüldü. SB'lerin an-*

tero-posterior, medio-lateral ve süperio-inferior uzunlukları ve hacimleri USG ile ölçüldü. KIBT ve USG ölçümleri istatistiksel olarak değerlendirildi. Bulgular: SF derinliği ile SB medio-lateral boyutu (p = 0.023), SF genişliği ve SB antero-posterior boyutu (p = 0.021), SF genişliği ve SB hacmi (p = 0.000) arasında istatistiksel olarak anlamlı pozitif korelasyonlar bulundu. Ancak SF derinliği ile SB hacmi arasında anlamlı bir ilişki bulunmadı (p=0,146). Sonuç: Alt çene posterior bölgede planlanan cerrahi işlemlerde özellikle implant uygulamalarında SF çok önemli bir alandır. SF derinliği ve genişliği, SB boyutlarıyla yakından ilişkilidir. USG ile iyonize radyasyon riski olmaksızın SB de net olarak incelenebilir. Anahtar Kelimeler: Submandibular Bez, Submandibuler Fossa, Ultrasonografi, Konik Işınlı Bilgisayarlı Tomografi, implant cerrahisi.

Ethics Committee Approval: The study protocol has been approved by the Local Research Ethics Committee's decision numbered 2021/58.

Informed Consent: Participants provided informed constent.

Peer-review: Externally peer-reviewed.

Author contributions: FC participated in designing the study. EAG participated in generating the data for the study. FC participated in gathering the data for the study. EAG participated in the analysis of the data. EAG wrote the majority of the original draft of the paper. FC participated in writing the paper. EAG has had access to all of the raw data of the study. EAG has reviewed the pertinent raw data on which the results and conclusions of this study are based. EAG, FC have approved the final version of this paper. EAG, FC guarantee that all individuals who meet the Journal's authorship criteria are included as authors of this paper.

Conflict of Interest: The authors declared that they have no conflict of interest.

Financial Disclosure: The authors declared that this study has not received any financial support.

References

1. Bayrak S, Demirturk-Kocasarac H, Yaprak E, Ustaoglu G, Noujeim M. Correlation between the visibility of submandibular fossa and mandibular canal cortication on panoramic radiographs and submandibular fossa depth on CBCT. Med Oral Patol Oral Cir Bucal 2018;23:e105. [CrossRef]
2. Kamburoğlu K, Acar B, Yüksel S, Paksoy CS. CBCT quantitative evaluation of mandibular lingual concavities in dental implant patients. Surg Radiol Anat 2015;37:1209-15. [CrossRef]
3. Sumer AP, Zengin AZ, Uzun C, Karoz TB, Sumer M, Danaci M. Evaluation of submandibular fossa using computed tomography and panoramic radiography. Oral Radiol 2015;31:23-7. [CrossRef]
4. de Souza LA, Souza Picorelli Assis NM, Ribeiro RA, Pires Carvalho AC, Devito KL. Assessment of mandibular posterior regional landmarks using cone-beam computed tomography in dental implant surgery. Ann Anat 2016;205:53-9. [CrossRef]
5. Bialek EJ, Jakubowski W, Zajkowski P, Szopinski KT, Osmolski A. US of the major salivary glands: anatomy and spatial relationships, pathologic conditions, and pitfalls. Radiographics 2006;26:745-63. [CrossRef]
6. Scarfe WC, Farman AG, Sukovic P. Clinical applications of cone-beam computed tomography in dental practice. J Can Dent Assoc 2006;72:75-80.
7. Kamburoğlu K, Kiliç C, Ozen T, Yüksel SP. Measurements of mandibular canal region obtained by cone-beam computed tomography: a cadaveric study. Oral Surg Oral Med Oral Pathol Oral Radiol Endod 2009;107:e34-42. [CrossRef]
8. Naitoh M, Katsumata A, Kubota Y, Hayashi M, Ariji E. Relationship between cancellous bone density and mandibular canal depiction. Implant Dent 2009;18:112-8. [CrossRef]
9. Ritter L, Mischkowski RA, Neugebauer J, Dreiseidler T, Scheer M, Keeve E, et al. The influence of body mass index, age, implants, and dental restorations on image quality of cone beam computed tomography. Oral Surg Oral Med Oral Pathol Oral Radiol Endod 2009;108:e108-16. [CrossRef]
10. de Oliveira-Santos C, Souza PH, de Azambuja Berti-Couto S, Stinkens L, Moyaert K, Rubira-Bullen IR, et al. Assessment of variations of the mandibular canal through cone beam computed tomography. Clin Oral Investig 2012;16:387-93. [CrossRef]
11. Arisan V, Karabuda ZC, Avsever H, Özdemir T. Conventional multislice computed tomography (CT) and cone-beam CT (CBCT) for computer-assisted implant placement. Part I: relationship of radiographic gray density and implant stability. Clin Implant Dent Relat Res 2013;15:893-906. [CrossRef]
12. Cassetta M, Stefanelli LV, Pacifici A, Pacifici L, Barbato E. How accurate is CBCT in measuring bone density? A comparative CBCT-CT in vitro study. Clin Implant Dent Relat Res 2014;16:471-8. [CrossRef]
13. Quirynen M, Mraiwa N, van Steenberghe D, Jacobs R. Morphology and dimensions of the mandibular jaw bone in the interforaminal region in patients requiring implants in the distal areas. Clin Oral Implants Res 2003;14:280-5. [CrossRef]
14. Parnia F, Fard EM, Mahboub F, Hafezeqoran A, Gavgani FE. Tomographic volume evaluation of submandibular fossa in patients requiring dental implants. Oral Surg Oral Med Oral Pathol Oral Radiol Endod 2010;109:e32-6. [CrossRef]
15. Zengel P, Schrötzlmair F, Reichel C, Paprottka P, Clevert DA. Sonography: the leading diagnostic tool for diseases of the salivary glands. Semin Ultrasound CT MR 2013;34:196-203. [CrossRef]
16. Stratemann SA, Huang JC, Maki K, Miller AJ, Hatcher DC. Comparison of cone beam computed tomography imaging with physical measures. Dentomaxillofac Radiol 2008;37:80-93. [CrossRef]
17. Kobayashi K, Shimoda S, Nakagawa Y, Yamamoto A. Accuracy in measurement of distance using limited cone-beam computerized tomography. Int J Oral Maxillofac Implants 2004;19:228-31.
18. Damstra J, Fourie Z, Huddleston Slater JJ, Ren Y. Accuracy of linear measurements from cone-beam computed tomography-derived surface models of different voxel sizes. Am J Orthod Dentofacial Orthop 2010;137:16.e1-6; discussion -7. [CrossRef]
19. Gandage SG, Kachewar SG. An Imaging Panorama of Salivary Gland Lesions as seen on High Resolution Ultrasound. J Clin Diagn Res 2014;8:Rc01-13. [CrossRef]
20. Isaacson TJ. Sublingual hematoma formation during immediate placement of mandibular endosseous implants. J Am Dent Assoc 2004;135:168-72. [CrossRef]
21. Niamtu J, 3rd. Near-fatal airway obstruction after routine implant placement. Oral Surg Oral Med Oral Pathol Oral Radiol Endod 2001;92:597-600. [CrossRef]
22. Çağlayan F, Ocak A, Sümbüllü MA. Supramandibular lymph nodes in dental patients by ultrasonography. Nobel Med 2019;15.
23. Philipsen HP, Takata T, Reichart PA, Sato S, Suei Y. Lingual and buccal mandibular bone depressions: a review based on 583 cases from a world-wide literature survey, including 69 new cases from Japan. Dentomaxillofac Radiol 2002;31:281-90. [CrossRef]
24. Alghamdi AS. Pain sensation and postsurgical complications in posterior mandibular implant placement using ridge mapping, panoramic radiography, and infiltration anesthesia. ISRN Dent 2013;2013:134210. [CrossRef]
25. Nilsun B, Canan B, Evren H, Kaan O. Cone-Beam Computed Tomography Evaluation of the Submandibular Fossa in a Group of Dental Implant Patients. Implant Dent 2019;28:329-39. [CrossRef]